AIChE

Reaction Rate Constant of CO_2 Hydrate Formation and Verification of Old Premises Pertaining to Hydrate Growth Kinetics

Sebastien Bergeron and Phillip Servio
Dept. of Chemical Engineering, McGill University, 3610 University Street, Wong Building, Montreal, Canada H3A 2B2

DOI 10.1002/aic.11601
Published online September 24, 2008 in Wiley InterScience (www.interscience.wiley.com).

Experimental data on the rate of carbon dioxide hydrate formation in a semibatch stirred-tank reactor was obtained using a particle-size analyzer capable of detecting particles as small as 0.6 nanometers in a closed-loop system. Experiments were carried out at temperatures between 275.3 and 279.4 K and pressures ranging from 2,014 to 3,047 kPa. The reaction rate constant of CO_2 hydrate formation was determined using a newly developed kinetic model independent of the dissolution rate at the vapor-liquid water interface. The average reaction rate constant determined experimentally was found to increase with temperature following an Arrhenius-type relationship, from 1.8×10^{-8} m/s to 1.8×10^{-7} m/s, over the 4-degree range investigated. Similarly, the reaction rate constant calculated from a population balance varied from 1.4×10^{-8} m/s to 1.7×10^{-7} m/s over the same temperature interval. The initial number of hydrate particles was calculated using the mole fraction of the gas hydrate former in the bulk-liquid phase at the onset of hydrate growth rather than the equilibrium solubility. The cumulative relative scattering was also compared to the derived count rate to determine whether or not the number of hydrate particles remained constant during the hydrate growth experiment. © 2008 American Institute of Chemical Engineers *AIChE J,* 54: 2964–2970, 2008

Keywords: gas hydrate, kinetics, reaction rate constant, particle-size analysis, crystallization

Introduction

Clathrate hydrates are nonstoichiometric crystalline compounds in which a gas or a volatile liquid molecule suitable for hydrate formation is enclosed in a network consisting of water molecules linked together through hydrogen bonding. The presence of the gas molecule stabilizes the water lattice via weak van der Waals forces. Three different structures can be found naturally and have been reported in the literature, including structure I (sI), structure II (sII) and structure H (sH) hydrate.[1] In particular, structure I hydrates contain 2 small cavities, and 6 large cavities per unit cell, as well as 46 water molecules.[1] Assuming full occupancy, it follows that there are 5.75 moles of water per mole of gas hydrate reformer. As an example, both carbon dioxide and methane form structure I hydrate, while propane forms structure II. Structure H needs two components and water, and an example of this is neohexane in the presence of methane.

A great deal of research is being conducted on gas hydrates due to their potential applications. Naturally occurring methane hydrates are seen as an alternate energy source.[2] Furthermore, it has been suggested that storage and transportation of natural gas[2] or liquefied petroleum gases[3] could be carried out in hydrated form, over more conventional methods such as liquefied natural gas or compressed natural gas. Carbon dioxide sequestration is also looked on

Correspondence concerning this article should be addressed to P. Servio at phillip.servio@mcgill.ca.

as a means to mitigate the global warming effect.[2] Moreover, hydrogen storage in hydrated form is currently studied for mobile applications.[4] Such promising new technologies are reasons why kinetic studies should be further investigated. In particular, an accurate value for the reaction rate constant of hydrate formation is required for proper reactor design aimed at large-scale hydrate production, such as three-phase slurry reactors.[5] The reaction rate constant is the sole parameter affecting any reactor throughput and conversion that remains constant on scale-up, as both heat and mass transfer effects will change.

Numerous studies have been performed to determine the reaction rate constant of hydrate formation in semibatch stirred-tank reactors. Vysniauskas and Bishnoi[6,7] first studied the kinetics of methane and ethane hydrate formation and concluded that the rate of formation was a function of the interfacial area, pressure, temperature and degree of supercooling.[6] Englezos et al.[8,9] followed with their pioneering work, in which they proposed a kinetic model for hydrate formation based on crystallization and two-film theory, with one adjustable parameter, i.e., the reaction rate constant. They studied the kinetics of methane and ethane hydrate formation, as well as their mixtures. Later on, Monfort and Nzihou[10] used a laser granulometer, capable of detecting particles with sizes between 5.6–564 μm, as well as the model of Englezos et al.[8] to study the kinetics of cyclopropane hydrate formation. Skovborg and Rasmussen[11] have suggested that hydrate growth is mass-transfer limited, where the transport of the gas molecules from the gas phase to the liquid-water phase is the rate-determining step. Using the model of Englezos et al.,[8] Chun and Lee[12] studied the kinetics of carbon dioxide hydrate formation, yielding a reaction rate constant in the order of 1×10^{-6} mol/(m^2 s MPa). Malegaonkar et al.[13] also studied the kinetics of carbon dioxide hydrate formation. They used a corrected version of the model of Englezos et al.[8] to account for a minor inconsistency, as well as a correction for the high-solubility of carbon dioxide in water, and concluded that the reaction rate constant of carbon dioxide hydrate formation was in the order of 1×10^{-4} mol/(m^2 s MPa). Mork and Gudmundsson[14] followed a similar approach to that of Skovborg and Rusmussen,[11] introducing a model for hydrate formation, based solely on mass transfer. Clarke and Bishnoi[15] studied the kinetics of carbon dioxide hydrate formation using an *in situ* particle-size analyzer, capable of detecting particles with chord lengths greater than 0.5 μm, and the model of Englezos et al.[8] Their results yielded a reaction rate constant in the order of 1×10^{-3} mol/(m^2 s MPa). More recently, Hashemi et al[16] concluded that hydrate kinetic models should be based on a concentration driving force. Using their new driving force and the model of Englezos et al.[8] they revisited the work of Clarke and Bishnoi,[15] and obtained a reaction rate constant for carbon dioxide hydrate formation in the order of either 1×10^{-5} m/s, or 1×10^{-8} m/s, using the surface area measured experimentally by Clarke and Bishnoi[15] and the one determined from a population balance, respectively. Based on their results, they concluded that a true reaction rate constant for hydrate formation has yet to be determined due to inaccurate surface area measurements.[16] Bergeron and Servio[17] used the driving force proposed by Hashemi et al,[16] and developed a new kinetic model for hydrate growth. Using such a model and a particle-size analyzer capable of detecting particles with a diameter as small as 0.6 nm, they studied the kinetics of propane hydrate formation, and obtained a reaction rate constant in the order of 1×10^{-7} m/s. Nevertheless, due to some ambiguity regarding the actual value of the dissolution rate at the vapor-liquid water interface of a system containing particles,[17,18] Bergeron and Servio[19] introduced an alternate formulation of their model, with a driving force based on the difference between the mole fraction of the gas hydrate former in the bulk-liquid phase, and that under hydrate-liquid water equilibrium. They also reported mole fraction measurements of the gas hydrate former in the bulk-liquid phase during hydrate growth. Their results showed that the concentration of the gas hydrate former remains constant in the bulk-liquid phase during hydrate growth, and can be used to better estimate the initial number of hydrate particles.[19] This work uses the model of Bergeron and Servio[19] to determine the reaction rate constant of carbon dioxide hydrate formation.

Experimental Setup

As shown on Figure 1, the current experimental setup consists of an isothermal/isobaric semibatch stirred-tank crystallizer, a gas supply reservoir for hydrate formation, and a *Zetasizer Nano ZS* particle-size analyzer (*Malvern Instruments*). The *Zetasizer Nano ZS* particle-size analyzer can detect particles with diameters between 0.6 and 6,000 nm, with a maximum uncertainty of 10 to 15% on the size obtained from the intensity distribution. Due to the use of Mie theory to convert the intensity distribution into a number distribution, spherical particles are assumed. In addition, the *Zetasizer Nano ZS* contains an internal cooling device to maintain the desired operating temperature inside the cell. Hydrates are formed in the 600 cm^3 internal volume stainless steel crystallizer (12,000 kPa pressure rating). A *PPI DYNA/MAG MM-006* mixer (0–2,500 rpm) has been mounted on top of the crystallizer to ensure sufficient mixing. Gas is supplied from the stainless steel reservoir (internal volume of 1,000 cm^3) using a *Baumann 51000 Series Low Flow* control valve. Part of the crystallizer liquid phase is continuously circulated from the crystallizer to the particle-size analyzer using a *LabAlliance Model 1500* dual piston pump and a custom flow-through cell (6,000 kPa pressure rating, *Hellma*). Both the crystallizer and the reservoir are submerged in a cooling bath composed of 10% glycol and water mixture controlled via a *Thermo NESLAB RTE Series* refrigerated bath. Temperature and pressure measurements are performed using standard resistance temperature devices ($\pm$0.3°C), and *Rosemount 3051S Series* pressure transducers with a reference accuracy of 0.04% of the span. The readouts are then recorded and displayed using the *National Instruments NI-DAQ 7* data acquisition device and the *LabVIEW* software. The *LabVIEW* interface was written to calculate the number of moles consumed at any time during the experiment using the Trebble-Bishnoi equation of state,[20] the gas reservoir pressure and temperature measurements, as well as the gas reservoir volume. The standard error propagation technique led to an uncertainty of 3×10^{-3} mol on the experimental mole consumption.

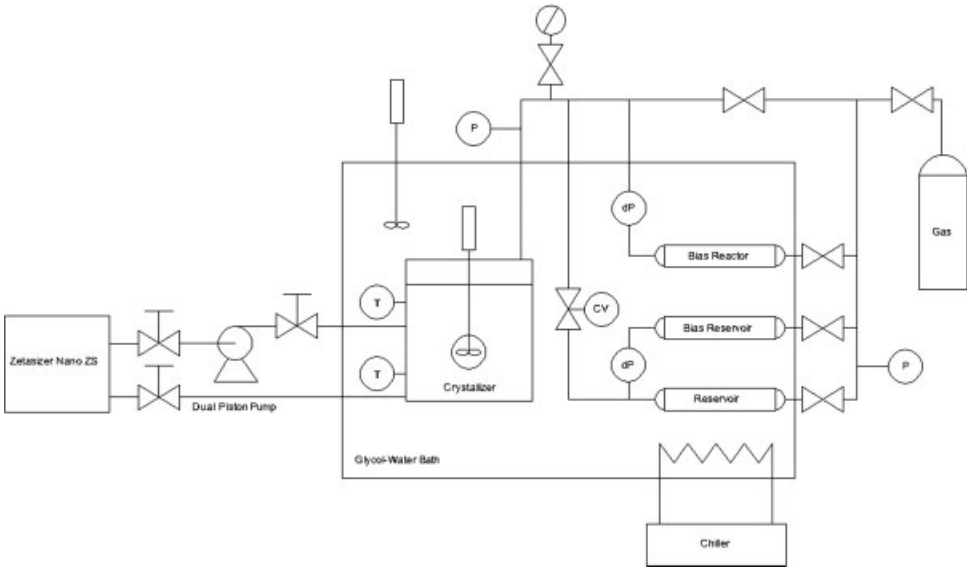

Figure 1. Simplified schematic of the experimental setup.

Experimental Procedure

Prior to any experiment, the crystallizer is cleaned using HPLC grade water and purged several times using the selected gas (carbon dioxide with *Coleman instrument grade* 99.99% purity). A syringe is used to introduce 180 mL of HPLC grade water in the crystallizer. Once thermal equilibrium has been reached, the crystallizer is pressurized above the hydrate-liquid water-vapor equilibrium pressure at the experimental temperature, but below the hydrate-liquid carbon dioxide-vapor equilibrium pressure (Figure 2). The dual piston pump is then started. Once the temperature in the reservoir and in the crystallizer has stabilized, both the data acquisition program and the crystallizer stirrer are started. The crystallizer stirrer is set to 750 rpm to minimize both heat and mass transfer effects. The onset of hydrate growth is identified by a sudden increase in the crystallizer liquid phase temperature, following which several particle-size distribution measurements are performed at different times to proper describe the growth stage of hydrate formation.

Kinetic Model

Bergeron and Servio[19] have proposed an alternate formulation of their kinetic model that is independent of the dissolution rate at the vapor-liquid water interface. Hence, according to their model, the rate at which gas is consumed for hydrate growth is given by[19]

$$\frac{dn}{dt} = \frac{V_L \rho_w}{MW_w} \frac{\left(x^l - x^{H-L}\right)}{\frac{1}{\pi \mu_2(t) k_r}} \tag{1}$$

where V_L, ρw and MW_w is the volume of liquid water, the density of water, and the molecular weight of water, respectively. In addition, x^l is the mole fraction of the gas hydrate former in the bulk-liquid phase at the experimental temperature and experimental pressure, while x^{H-L} is the solubility of the gas hydrate former under hydrate-liquid water equilibrium at the experimental temperature and experimental pressure. In their work,[19] Bergeron and Servio concluded that the mole fraction of the gas hydrate former in the bulk-liquid phase remains constant during hydrate growth. Moreover, μ_2 is the second moment of the particle-size distribution, and k_r is the reaction rate constant of hydrate formation. Note that a detailed derivation of Eq. 1, and its parameters can be found elsewhere.[17,19]

As mentioned previously, the model of Bergeron and Servio[19] was proposed due to the difficulty in measuring an accurate value for the dissolution rate at the vapor-liquid water interface. In previous kinetic studies,[8,11–13,15] researchers used the value obtained from solubility experiments, where the dissolution rate was measured in a system under vapor-liquid water equilibrium conditions. Hence, no hydrate particles were present and it seemed legitimate to assume that both the vapor-liquid water interfacial area, and the mass-transfer coefficient at the interface remained constant. However, in their recent study, Bergeron and Servio[17] suggested that due to the presence of hydrate particles during

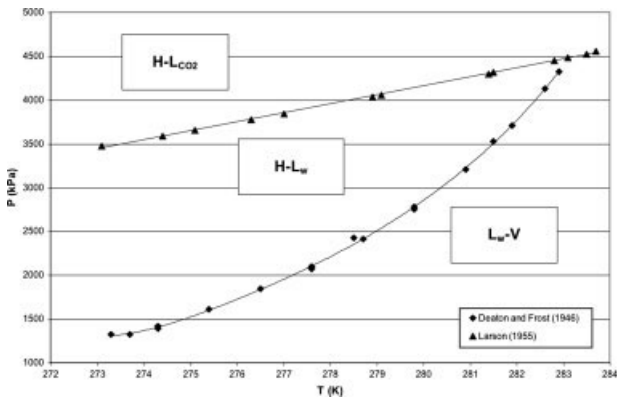

Figure 2. Carbon dioxide-water phase diagram using the experimental data of Deaton and Frost and Larson.[28]

hydrate growth experiments, either the vapor-liquid water interfacial area, or the mass-transfer coefficient at the interface, or both, could vary from the values measured through typical solubility experiments. These conclusions were also based on the work of Kluytmans et al.[18] performed with systems containing carbon particles. Since the driving force used in Eq. 1 is based on the mole fraction of the gas hydrate former in the bulk-liquid phase, the model is independent of the dissolution rate and removes any ambiguity regarding such an issue.

The optical properties required by the particle-size analyzer, namely the refractive index and the absorption of carbon dioxide hydrates, were obtained from the work of Bonnefoy et al.[21] and Warren,[22] respectively. In the latter case, since only an order of magnitude estimate was required, carbon dioxide hydrates were assumed to have absorption values similar to that of ice Ih (hexagonal ice), which is the most common solid form of water.[1] Such an assumption is based on the fact that hydrates are comprised of roughly 85% water on a molecular basis. Furthermore, x^l is obtained from the work of Bergeron and Servio,[19] while x^{H-L} is obtained from the model of Hashemi et al.[23] As for μ_2, it can be obtained either experimentally, using the particle-size analyzer, or from a semitheoretical approach, using a population balance. In the latter case, assuming a constant volume, a size independent growth and a constant number of particles, the population balance yields[24]

$$\frac{d\varphi}{dt} + \frac{d(G\varphi)}{dL} = 0 \tag{2}$$

where G is the growth rate, and L the hydrate diameter.

Using the mean diameter obtained for each particle-size distribution measurement performed, an expression for the growth rate can be obtained using the following

$$G = \frac{dL}{dt} \tag{3}$$

Equation 2 can then be transformed into a set of differential equations and performing the moment transformations[24] leads to

$$\mu_0 = \mu_0^0 \tag{4}$$

$$\mu_1 = \mu_0^0 Gt + \mu_1^0 \tag{5}$$

$$\mu_2 = \mu_0^0 G^2 t^2 + 2\mu_1^0 Gt + \mu_2^0 \tag{6}$$

where μ_0, μ_1 and μ_2 are the zeroth, first and second moment, respectively. The initial number of particles is discussed in the subsequent section, while μ_1^0 and μ_2^0 are given by

$$\mu_1^0 = L_c \mu_o^0 \tag{7}$$

$$\mu_2^0 = L_c^2 \mu_o^0 \tag{8}$$

where L_c is the critical nuclei diameter and is obtained by performing a size distribution measurement at the onset of hydrate growth.

Hence, incorporating Eqs. 6, 7 and 8 into Eq. 1 allows for the determination of the reaction rate constant using a population balance

$$\frac{dn}{dt} = \frac{V_L \rho_w}{MW_w} \frac{\left(x^l - x^{H-L}\right)}{\frac{1}{\pi\left(\mu_0^0 G^2 t^2 + 2L_c \mu_o^0 Gt + L_c^2 \mu_o^0\right) k_r}} \tag{9}$$

Number of Hydrate Particles

Bergeron and Servio[19] also suggested that the initial number of hydrate particles should be calculated using the number of moles of the gas hydrate former in the bulk-liquid phase at the onset of hydrate growth. Accordingly, the initial number of hydrate particles is given by[19]

$$\mu_0^0 = \frac{6MW_H(n_{tb} - n^l)}{\eta\pi V_L \rho_H L_c^3} \tag{10}$$

where MW_H and ρ_H is the molecular weight and density of the hydrate, respectively. The number of moles of gas dissolved at turbidity is given by n_{tb}, while η is the number of moles of gas per mole of hydrate. Note that full occupancy of both the small and large cavity was assumed in the calculations.

There is some controversy regarding the assumption that the number of hydrate particles remains constant during the growth stage. Englezos et al.[8] considered secondary nucleation, but concluded that it was negligible since hydrate crystals are very small. Herri et al.[25,26] studied the role of primary nucleation, secondary nucleation, breakage, attrition and agglomeration on methane hydrate crystallization. Their turbidimetry measurements allowed for the detection of particles with sizes between 10 and 150 μm. They concluded that a simplified model of primary nucleation and growth was sufficient to explain the effect of the stirring rate on the initial mean diameter and the initial number of particles.[26] They also suggested that secondary nucleation could explain the behavior of crystallization at high-stirring rates.[26] The authors of this work are skeptical regarding the possibility of secondary nucleation due to the intense mixing (750 rpm) occurring in the current semibatch stirred-tank reactor. For secondary nucleation to proceed, local supersaturation of the gas hydrate former in the bulk-liquid phase would have to persist long enough for new nuclei to form. On the other hand, we believe it is more likely that existing hydrate particles will consume any excess in gas.

In their extensive literature review of existing hydrate growth kinetic models, Ribeiro and Lage[27] concluded that future models should account for the particle-size distribution, including particle agglomeration and breakage. In an attempt to determine if particle breakage, agglomeration and/or attrition play a significant role, a new technique was developed to assess whether or not the number of hydrate particles remains constant during hydrate growth. First, the *Zetasizer Nano ZS* particle-size analyzer provides the derived count rate for each size distribution measurement performed. Such a count rate, which is normalized for the cell position and the attenuation used, represents the number of photons detected by the particle-size analyzer.

The software package used with the *Zetasizer Nano ZS* particle-size analyzer also includes a utility that uses Mie theory to predict the relative scattering per particle for a given set of optical properties. Hence, for the size range detectable by the *Zetasizer Nano ZS*, namely from 0.6 to

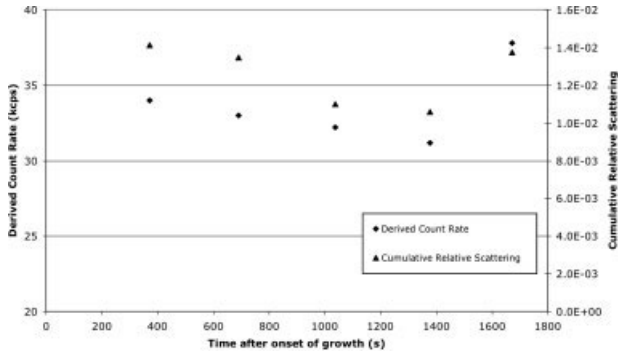

Figure 3. Comparison of the derived count rate and the cumulative relative scattering at 279.2 K and 3,047 kPa.

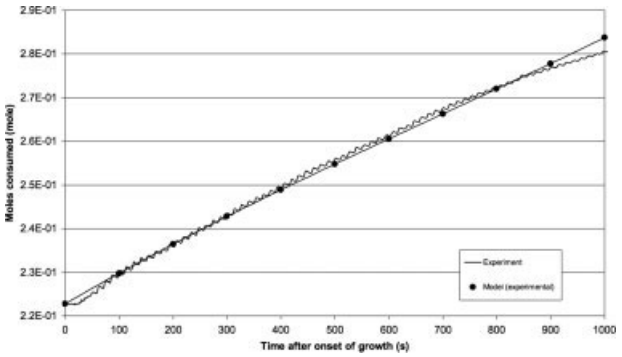

Figure 5. Comparison between the experimental mole consumption and the model predictions at 279.2 K and 3,047 kPa.

6,000 nm, the relative scattering distribution can be obtained. For certain size ranges, e.g., from approximately 1 to 240 nm, Mie theory predicts an increasing relative scattering per particle. However, for other size ranges, e.g., from approximately 240 to 340 nm, Mie theory predicts a decreasing relative scattering per particle. It follows that depending on the size range the hydrate particles are in, the relative scattering per particle will either increase or decrease from one measurement to the other. Using the various size distributions obtained experimentally, the cumulative relative scattering is calculated for each measurement. Hence, comparing the trend of the cumulative relative scattering to the derived count rate can shed light on the number of particles. In the event that both the derived count rate, and the cumulative relative scattering follow the same trend over time, it can be assumed that the number of particles remains constant. Even though it is impossible to confirm with certainty such an assumption, a significant change in the number of hydrate particles would lead to opposite trends for the derived count rate and the cumulative relative scattering.

Results

Several experiments were performed over a 4-degree interval to determine the reaction rate constant of carbon dioxide hydrate formation. As mentioned previously, the reaction rate constant was determined using both Eqs. 1 and 9, to compare the experimental value to the semitheoretical one (population balance). For each experiment, the derived count rate was compared to the cumulative relative scattering to determine if the number of hydrate particles remains constant during the growth stage. Figure 3 shows such a comparison at 279.2 K and 3,047 kPa. It can be seen that over the entire duration of the experiment, both the derived count rate and the cumulative relative scattering follow the same trend, fostering the hypothesis that the number of hydrate particles remains constant. Figure 4 shows the second moment obtained experimentally using the particle-size analyzer at 279.2 K and 3,047 kPa. As expected, hydrate particles grow with time, resulting in an increase in the total surface area, and, thus, an increase in the second moment. Both Eqs. 1 and 9 were integrated and compared to the experimental mole consumption. The reaction rate constant was regressed using the Gauss-Newton method with Levenberg-Marquardt's modification. Figure 5 shows the comparison between the experimental mole consumption and the model predictions at 279.2 K and 3,047 kPa. For those conditions, a reaction rate constant of 1.62×10^{-7} m/s, was obtained experimentally, while a value of 1.44×10^{-7} m/s was obtained using a population balance. Clearly, a very good agreement exists between the experimental data and the model, with an average absolute relative error of 0.3% for the experimental reaction rate constant and 0.7% for the semitheoretical one.

Table 1 lists the average reaction rate constant obtained for various temperatures, based on replicates. As it can be seen from Figure 6, the reaction rate constant increases with temperature and follows an Arrhenius-type relationship. To the best of our knowledge, we are the first to report such a trend for the reaction rate constant of any hydrate former.

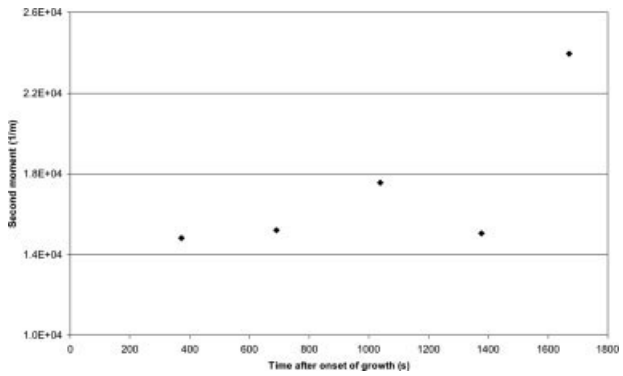

Figure 4. Experimental second moment of the particle-size distribution at 279.2 K and 3,047 kPa.

Table 1. Reaction Rate Constant of CO_2 Hydrate Formation

Temperature (K)	Experimental Reaction Rate Constant ($\times 10^{-8}$ m/s)	Semitheoretical Reaction Rate Constant ($\times 10^{-8}$ m/s)
275.5	1.8 ± 0.3	1.4 ± 0.2
277.5	4.5 ± 1.0	4.1 ± 0.4
279.3	18.0 ± 2.0	17.0 ± 2.0

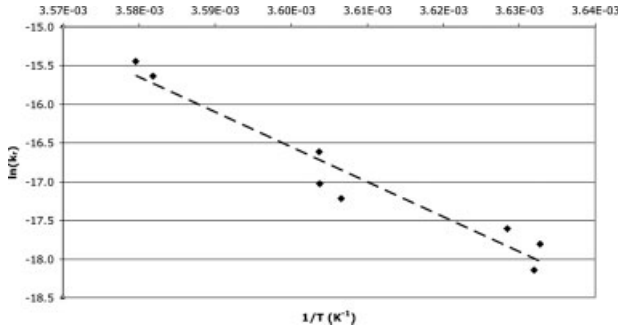

Figure 6. Reaction rate constant of CO_2 hydrate formation over a 4-degree interval.

Indeed, some researchers[8,13,15] have reported a minimum value for the reaction rate constant of several hydrate formers around 277 K, while Englezos et al.[8] highlighted that such a trend coincides with the highest density of water. The authors are skeptical regarding such an implication since no such trend was observed in the current study. Moreover, the change in water density is not significant over the temperature interval investigated. Finally, all the studies reporting such a minimum in the reaction rate constant incorporated the model of Englezos et al.[8] and two-film theory, while the current study is the first to use a different approach.

Since previous studies[12,13,15] for the reaction rate constant of carbon dioxide hydrate formation were based on a fugacity driving force, the current values can only be compared to the work of Hashemi et al.[16] who revisited the work of Clarke and Bishnoi[15] using a concentration driving force and the model of Englezos et al.[8] The values reported in this work for the reaction rate constant of CO_2 hydrate formation at 277.5 K, namely 4.5×10^{-8} m/s, and 4.1×10^{-8} m/s depending on the method used, are in relative agreement with the value reported by Hashemi et al.[16] using a population balance at 277.15 K, i.e., 1.20×10^{-8} m/s.

Conclusion

The reaction rate constant for carbon dioxide hydrate formation was successfully determined over a 4-degree interval. The reaction rate constant determined experimentally was found to increase with temperature following an Arrhenius-type relationship, from 1.8×10^{-8} m/s to 1.8×10^{-7} m/s over the 4-degree range investigated. Similarly, the reaction rate constant calculated from a population balance varied from 1.4×10^{-8} m/s to 1.7×10^{-7} m/s over the same temperature interval.

Acknowledgments

The authors are grateful to the Natural Sciences and Engineering Research Council of Canada for financial assistance, as well as the Canada Research Chair program and the Canadian Foundation for Innovation.

Notation

μ_0^0 = initial number of hydrate particles
μ_0 = zeroth moment of the particle-size distribution, m^{-3}
μ_1 = first moment of the particle-size distribution, m^{-2}
μ_2 = second moment of the particle-size distribution, m^{-1}
ρ = density, g m^{-3}
$\pi = Pi$
η = gas molecules per hydrate molecule
ϕ = particle-density distribution, m^{-4}

Letters

k_r = reaction rate constant, m s^{-1}
G = growth rate, m s^{-1}
L = hydrate diameter, m
Lc = critical nuclei diameter, m
MW = molecular weight, g mol^{-1}
n = moles, mol
P = pressure, kPa
t = time, s
T = temperature, K
V_L = volume of liquid, m^3
x = mole fraction

Subscripts

exp = experimental
tb = turbidity
W = water

Supercripts

H = hydrate
l = bulk liquid
H – L = hydrate-liquid water
L – V = vapor-liquid water
V = vapor

Literature Cited

1. Sloan ED, Koh CA. *Clathrate Hydrates of Natural Gases*. 3rd ed. CRC Press, 2007.
2. Chatti I, Delahaye A, Fournaison L, Petitet J-P. Benefits and drawbacks of clathrate hydrates: a review of their areas of interest. *Ener Conv Manage*. 2005;46:1333–1343.
3. Giavarini C, Maccioni F, Santarelli ML. Formation kinetics of propane hydrates. *Ind Eng Chem Res*. 2003;42:1517–1521.
4. Mao WL, Koh CA, Sloan ED. Clathrate hydrates under pressure. *Phys Today*. 2007:42–47.
5. Hashemi S, Macchi A, Servio P, Dynamic Simulation of Gas Hydrate Formation in an Agitated Three-Phase Slurry Reactor. In: 2007 ECI Conference on The 12th International Conference on Fluidization - New Horizons in Fluidization Engineering, Vancouver, Canada; 2007:329–336.
6. Vysniauskas A, Bishnoi PR. A kinetic study of methane hydrate formation. *Chem Eng Sci*. 1983;38:1061–1072.
7. Vysniauskas A, Bishnoi PR. Kinetics of ethane hydrate formation. *Chem Eng Sci*. 1985;40:299–303.
8. Englezos P, Kalogerakis N, Dholabhai PD, Bishnoi PR. Kinetics of formation of methane and ethane gas hydrates. *Chem Eng Sci*. 1987;42:2647–2658.
9. Englezos P, Kalogerakis N, Dholabhai PD, Bishnoi PR. Kinetics of gas hydrate formation from mixtures of methane and ethane. *Chem Eng Sci*. 1987;42:2659–2666.
10. Monfort JP, Nzihou A. Light scattering kinetics study of cyclopropane hydrate growth. *J Crystal Growth*. 1993;128:1182–1186.
11. Skovborg P, Rasmussen P. A mass transport limited model for the growth of methane and ethane gas hydrates. *Chem Eng Sci*. 1994;49:1131–1143.
12. Chun M-K, Lee H. Kinetics of formation of carbon dioxide clathrate hydrates. *Kor J Chem Eng*. 1996;13:620–626.
13. Malegaonkar MB, Dholabhai PD, Bishnoi PR. Kinetics of carbon dioxide and methane hydrate formation. *Can J Chem Eng*. 1997;75:1090–1099.
14. Mork M, Gudmundsson JS. Hydrate Formation Rate in a Continuous Stirred Tank Reactor: Experimental Results and Bubble-to-Crystal Model. Proceedings of the Fourth International Conference on Gas Hydrates. Yokohama, Japan; May 19–23, 2002.

15. Clarke M, Bishnoi PR. Determination of the intrinsic kinetics of CO_2 gas hydrates formation using in situ particle size analysis. *Chem Eng Sci*. 2005;60:695–709.
16. Hashemi S, Macchi A, Servio P. Gas hydrate growth model in a semi-batch stirred tank reactor. *Ind Eng Chem Res*. 2007;46:5907–5912.
17. Bergeron S, Servio P. Reaction rate constant of propane hydrate formation. *Fluid Phase Equilib*. 2008;265:30–36.
18. Kluytmans JHJ, Wachem BGMv, Kuster BFM, Schouten JC. Mass transfer in sparged and sittred reactors: influence of carbon particles and electrolyte. *Chem Eng Sci*. 2003;58:4719–4728.
19. Bergeron S, Servio P. CO_2 and CH_4 mole fraction measurements during hydrate growth in a semi-batch stirred tank reactor and its significance to kinetic modeling. *Fluid Phase Equilib*. 2008 (submitted).
20. Trebble MA, Bishnoi PR. Development of a new four-parameter cubic equation of state. *Fluid Phase Equilib*. 1987;35:1–18.
21. Bonnefoy O, Gruy F, Herri J-M. A priori calculation of the refractive index of some simple gas hydrates of structures I and II. *Mat Chem Phys*. 2005;89:336–344.
22. Warren SG. Optical constants of ice from the ultraviolet to the microwave. *Applied Optics*. 1984;23:1206–1225.
23. Hashemi S, Macchi A, Bergeron S, Servio P. Prediction of methane and carbon dioxide solubility in water in the presence of hydrate. *Fluid Phase Equilib*. 2006;246:131–136.
24. Kane SG, Evans TW, Brian PLT, Sarofim AF. Determination of the kinetics of secondary nucleation in batch crystallizers. *AIChE J*. 1974;20:855–862.
25. Herri JM, Gruy F, Pic JS, Cournil M, Cingotti B, Sinquin A. Interest of in situ turbidimetry for the characterization of methane hydrate crystallization: Application to the study of kinetic inhibitor. *Chem Eng Sci*. 1999;54:1849–1858.
26. Herri JM, Pic JS, Gruy F, Cournil M. Methane hydrate crystallization mechanism from in-situ particle sizing. *AIChE. J*. 1999;45:590–602.
27. Ribeiro CP, Lage PLC. Modelling of hydrate formation kinetics: State-of-the-art and future directions. *Chem Eng Sci*. 2008;63:2007–2034.
28. Sloan ED. *Clathrate Hydrates of Natural Gases*. 2nd ed. New York: Marcel Dekker, Inc; 1998.

Manuscript received Apr. 12, 2008, and revision received Jun. 18, 2008.